GEM TN-92-54

The GEM Central Tracker: Design Issues

Geoffrey B. Mills
Los Alamos National Laboratory

November 14, 1991

Abstract:

A discussion of design issues of the GEM central tracker is given. General features of the tracker performance are discussed in the context of the SSC environment at luminosities of $10^{33}cm^{-2}s^{-1}$ and $10^{34}cm^{-2}s^{-1}$.

The GEM Central Tracker: Design Issues

by
Geoffrey B. Mills
Los Alamos National Laboratory
November 14, 1991

Abstract

A discussion of design issues of the GEM central tracker is given. General features of the tracker performance are discussed in the context of the SSC environment at luminosities of $10^{33}cm^{-2}s^{-1}$ and $10^{34}cm^{-2}s^{-1}$.

Introduction

In this Document I would like to address some of the issues which relate to the design of the GEM central tracker (CT). The GEM CT is in all likelihood the most challenging subsystem in the GEM detector. The tracker must simultaneously deal with a high radition environment, large number of background tracks, a short path length for momentum measurement, and be affordable within the GEM budget. First I address the physics goals of the GEM CT, followed by a description of the environment in which it will live, and finally I discuss the expected performance of a strawman design which is being contemplated at the curren time such as the occupancy levels, the momentum resolution, and the impact parameter resolution.

Physics Goals

The physics goals of the GEM CT follow closely the needs of the overall detector. The primary goals of the detector are to be able to identify high P_t leptons and photons. This ability is critical in identifying important reactions such as $H^0 \rightarrow 4$ leptons and other high P_t phenomena. The CT will play a central role in electron identification and in determining the sign of the charge of electrons. Charge sign determination requires good momentum resolution while efficient electron identification requires good pattern recognition and low occupancy for high efficiency. In addition, channels such as $H^0 \rightarrow \gamma\gamma$ require the tracker to independently measure the multiplicity of each of the primary vertices in the event. This requires good pattern recognition and Z vertex resolution in the range of 1mm or better.

Also important to the GEM physics goals is the ability to identify quark jets via the long decay lengths of the B and D mesons. High efficiency (>50%) with high rejection factors (>100) can be achieved under certain conditions. This ability is extremely useful in obtaining clean samples of top and bottom events, and, in addition, shed light on the nature of Higgs candidate couplings.

The potential to identify τ leptons is also a powerful enhancement to the overall physics capability of the GEM detector. This channel could in principle offer a complementary handle to the muon and electron on fundemental physics topics involving Higgs, Z^0, and $W^{\pm}$ decays.

Event Backgrounds and the SSC Environment

The SSC experimental environment is one of the most ambitious in high energy physics. A summary of the parameters is shown in Table 1. The luminosity is 10^{33} $cm^{-2}s^{-1}$ with a bunch crossing frequency of 62.5 MHz. This corresponds to 0.016 mb^{-1} integrated luminosity per crossing. The proton-proton inelastic cross section is roughly 100mb at this energy giving rise to a 'minimum bias' event background of on the average 1.6 events. These events will overlay any rare physics process of interest with approximately $dN_{ch}/d\eta d\phi = 1.2$ tracks per unit area in η-ϕ space. In addition to this, for hard scattering

processes, there is an additional background due to the remnants of the protons that had the hard collision. This, combined with the minimum bias collisions, gernerates a total background of $dN_{ch}/d\eta d\phi = 4.1$ tracks per unit area in η-ϕ space. It is interesting to note that one expects a total of 1.6+1=2.6 collisions for rare processes (see the discussion in Appendix 1).

Table 1. SSC operational parameters

Luminosity	10^{33} $cm^{-2}s^{-1}$
Crossing Frequency	62.5 MHz
Minimum Bias Cross Section	90-100 mb
$\frac{dN_{ch}}{d\eta d\phi}$ for Minimum Bias Event	1.2 charged particles
Minimum Bias Events per Crossing	1.6
$\frac{dN_{ch}}{d\eta d\phi}$ for one beam crossing	1.9 charged particles
$\frac{dN_{ch}}{d\eta d\phi}$ for 300GeV Higgs Events	4.1 charged particles

The above backgrounds are for the charged primary tracks only. In addition, there is a contribution from particles which loop in the magnetic field, secondary delta-ray production, particle decays, and photon conversions which could add as much as 2-4 to $dN_{ch}/d\eta d\phi$. Thus we are left with the prospect of a background of $dN_{ch}/d\eta d\phi = 6$-8 in physics processes of interest such as Higgs production and top production.

Figure 1. shows several distributions for minimum bias triggers. This figures were generated with program PYTHIA. The average number of tracks into the region -2.5<h<2.5 is shown in the first graph while the average number of photons(from π^0 decays) is shown in the next graph. The average number of tracks(photons) is 60(70). The corresponding transverse momentum distributions are shown on the next two graphs. The charged tracks(photons) have an average p_t of 495(271)MeV/c respectively. Figure 2 shows the same distributions for Higgs(M_H=300GeV) events where the Higgs daughters have not been included in the plots. It is clear that the hard scattering processes have a much higher underlying track background. The Higgs interaction contributes roughly 1.9

to $dN_{ch}/d\eta d\phi$. Figure 3 shows several distributions for the Higgs decay products where the reaction proceeds as $H_0 \rightarrow Z_0Z_0 \rightarrow$ 4 leptons . It is clear that one needs η coverage to ± 2.5 in order to have reasonable efficiency for finding this important reaction.

Radiation Dose Levels

The radiation dose in the central tracker volume is composed of three parts, the primary ionizing tracks which come from the interaction region, the albedo neutrons which come from the calorimetry, and everything else which includes secondaries, loopers, albedo photons etc.. In general the following numbers are valid at $\eta = 0$, at $\eta = \pm 2.5$ the dose levels increase by roughly 50% due to two factors, the relativistic rise of the specific energy loss due to higher energy particles in the forward directions and also due to the increase in particle density in pseudorapidity the forward directions.

The yearly primary charged particle flux (at $\eta = 0$) is given by :

$$\frac{dN_{ch}}{dA} = \frac{10^{15}\ \text{particles}}{R_{\perp}^2[\text{cm}]}$$

This flux is the number of particles through a normal area element dA at perpendicular radius $R_{\perp}$ per SSC year (10^7s at $L=10^{33}$). The dose is calculated by taking the specific energy loss for minimum ionizing particles in light elements [1] of roughly

$$\frac{dE}{dx} = 1.8\ \frac{\text{MeV-cm}^2}{\text{g}} = 2.88 \times 10^{-8}\text{Rad-cm}^2$$

to obtain :

$$\text{Yearly dose from charged particles} = \frac{dE}{dx}\ \frac{dN_{ch}}{dA} = \frac{29\ \text{MRad}}{R_{\perp}^2[\text{cm}]}$$

In addition there is a contribution of albedo neutrons which from the calorimetry. This flux can be reduced by almost an order of magnitude [2] to a yearly flux level of 1.7×10^{12}n(1MeV)/cm^2 by using a borated polyethylene shield between the calorimetry and the tracker. The neutrons are only damaging to the silicon part of the tracker, as the IPC gas will have a very low interaction probability with the neutrons. The damage factor

which is applied for neutrons assumes that a 1MeV neutron gives the same damage as 1 minimum ionizing particle does.

$$\text{Yearly dose from neutrons} = \frac{dE_n}{dx}\ \frac{dN_n}{dA} = .049 \text{ MRad}$$

There is in addition a factor due to secondaries and loopers which needs to be included. At this moment this has not been calculated explicitly but for our purposes it is assumed to be L=1.5. The total dose relevant to silicon damage is then given by the following formula:

$$\text{Total dose} = \left(\frac{29 \cdot L}{R_\perp{}^2[\text{cm}]} + .049\right) \text{MRad}$$

In general, radiation hardened silicon strip devices can survive to the dose D=3 MRad level[3] and the same is true of typical radiation hardened CMOS and bipolar technologies. Given this upper bound and system lifetime, T, one can determine a minimum radius for the silicon system.

$$R_\perp{}^{min} = \sqrt{\frac{29.0 \cdot L \cdot T}{D - .049 \cdot T}} = \begin{cases} 13.1\text{cm } T=10 \text{ years} \\ 8.9\text{cm } T=5 \text{ years} \end{cases}$$

Figure 4 shows the dependence of the 3Mrad dose lifetime as a function of $R_\perp$.

In the IPC system the concern is the amount of charge per unit length which one may accumulate on a given wire. This is a straight forward calculation once one knows the charged particle flux through a wire given :the wire gain G_{wire} , the chamber thickness $t_{chamber}$, and the number of ion pairs created per unit length dN_{ion}/dx $w_{chamber}$:

$$\lambda = e\, G_{wire}\, t_{chamber} \frac{dN_{ion}}{dx}\ w_{chamber} \frac{dN_{ch}}{dA}\ L$$

$$= 1.6\text{x}10^{-19} \text{ x } 10^4 \text{ x } .5\text{x } 30 \text{ x } .25 \text{ x } \frac{10^{15}}{R_\perp{}^2[\text{cm}]} \text{ x } 1.5$$

$$= \frac{6.0}{R_\perp{}^2[\text{cm}]} \text{ C/cm per year}$$

Typical large scale systems have survived in excess of 0.1 C/cm which would imply a minimum radius of around 25 cm for a 10 year lifetime. Small bench-top tests have

demonstrated[4] the operation of chambers to higher dose levels of as much as 10C/cm. It remains to be seen if these results can be extrapolated to larger systems. At luminosities of$10^{34}cm^{-2}s^{-1}$ the situation is such that the chamber would have to tolerate nearly 1.0 C/cm in order to survive at 25 cm.

Strawman Design

The strawman design which I use in further calculations is based on a silicon strip tracker that is surrounded by a IPC (Interpolating Pad Chamber). The zeroth order design is shown in Figure 5, 6, and 7.

Silicon

The design philosophy for this system is to maintain at least a six double- layer coverage in the pseudorapidity range [$-2.5<\eta<2.5$]. The silicon strip readout pitch is maintained at 50μm in all layers. In addition, radiation damage constrains the minimum radius of the system to be 10cm from the beam axis if one accepts a 5 year lifetime for the inner-most silicon ladders. The radius of the outer layer is set by cost considerations to 220mm. These and other parameters are tabulated in the Figure 8.

In Figures 5 and 6b one sees that the silicon barrel ($-1.5<\eta<1.5$) is made of six layers of silicon ladders. Each ladder is built from two sensor layers of single sided silicon sensors, one layer that has strips parallel to the Z axis and one layer that has a 5 mrad stereo angle with respect to the Z axis. The ladder sensor layer has a length of 120mm and a width of 33 mm, and is constructed from two 60mmx33mm silicon sensors which are wire-bonded in the center to form contiguous 120mm strips. Each ladder layer measures a space point with a resolution of roughly10μm in r-ϕ and 2-3mm in r-z.

The forward region of the the silicon tracker is shown in Figures 5 and 6a. In the forward regions the silicon tracker is made of 12 disks of pie slice shaped ladders that vary in length from 40mm to 120mm. Each disk measures a space point as described for the barrel region. Any track that comes from the origin will cross at least 6 double-layers of silicon ladders.

IPC

The Interpolating Pad Chamber (IPC) system is constructed from three super-layers each of which have three IPC layers for a total of nine layers of IPC as shown in Figures 5 and 7. The design philosophy in this system is to maintain a uniform $\Delta\eta\Delta\phi$ of coverage of .001 for each pad in the system, regardless of radial or angular position.

The pad width in the chamber is set by the constraint on the r-ϕ resolution of 50μm. The resolution is assumed to be approximately 1 per cent of the pad width which leads to a pad width of 5mm. The r-z extent of the pad is then adjusted to maintain $\Delta\eta\Delta\phi = .001$. This leads to pad lengths in the range from 5mm up to 100mm. The pad system parameters are tabulated in Figure 9 which contain tables of IPC parameters that relate to geometrical configuration and occupancies.

Occupancy Considerations

An interesting parameter is the occupancy of a given tracker element. This is often misleading as to its implications in track finding, but, never the less, it is useful in giving some upper bounds on tracker element sizes. Figures 8 and 9 are show tables of the expected primary track crossings for various cells in the Silicon system and the IPC system. These numbers represent a lower bound to the number of tracking cells which are hit on an average event. In general one can represent the track density in interesting physics processes as :

$$\frac{dN_{ch}}{d\eta d\phi} = (4.1 + 1.6\,(N_{bunch}-1))\times L = \begin{cases} 6.2 \text{ Silicon} \\ 10.0 \text{ IPC} \end{cases}$$

where L is a factor for secondaries and loopers taken to be 1.5 here. The goal is to keep the cell size small so that the average number of tracks in the cell is less than 0.01 . This will require a $\Delta\eta\Delta\phi$ extent of less than 1.6×10^{-3} in the silicon and 1.0×10^{-3} in the IPC.

In the silicon system the occupancy numbers vary due to the fixed size of the silicon sensor and ladder structure. The primary track occupancies varies from 8.1×10^{-4} (inner barrel at η=0.0) to 9.2×10^{-5} (outer barrel at $\eta=\pm1.4$). These are all listed in the table in Figure 8. Another interesting quantity is the 'space point' occupancy which can be defined as the occupancy for the minimum size cell that would allow unambiguous space point reconstruction. This varies from 7.1×10^{-4} in the forward region to 9.8×10^{-3} in the inner barrel cylinder at η=0.0 .

In the IPC system the 'space point' is determined by the pad $\Delta\eta\Delta\phi$ times the number of pads which one chamber wire crosses, roughly :

$$\langle Nch \rangle = \frac{dN_{ch}}{d\eta d\phi} \times \Delta\eta\Delta\phi \times \frac{L_{wire}}{w_{pad}} = 10.x.001x\frac{180mm}{5mm} = 30\ \%$$

so that

$$\text{IPC Space Point Occupancy} = 1 - e^{-\langle Nch \rangle} = 26\%$$

These ocuppancy numbers, including the effects of integration time, loopers, and the background physics events are summarized in Table 2.

Table 2. Occupancies in the Central Tracker

Silicon	$\Delta\eta\Delta\phi$ cell	Occupancy (%)	Fraction of Time Dead(%)	Space Point Occupancy(%)
$L=10^{33}cm^{-2}s^{-1}$	0.9-8.0x 10^{-4}	0.06-0.22	.6-2.2	.72-2.6
$L=10^{34}cm^{-2}s^{-1}$	"	0.26-2.2	2.6-22.2	3.1-23.2
IPC				
$L=10^{33}cm^{-2}s^{-1}$	.001	1.0	0	26.0
$L=10^{34}cm^{-2}s^{-1}$	"	4.9	0	78.0

At a higher luminosity of $10^{34}cm^{-2}s^{-1}$ the silicon is not expected to survive however the IPC system might possibly be of use. In this case we would have the following track densities:

$$\frac{dN_{ch}}{d\eta d\phi} = (18 + 16\,(N_{bunch}-1))x\ L = \begin{cases} 27 \text{ Silicon} \\ 51 \text{ IPC} \end{cases}$$

The raw occupancies would be at the level of 5.0% (.05) and one would have to fold in the effect of neighboring channel(~2) and track curvature(~3) to end up with a pseudo stiff track finding efficiency of (i.e., the probability that a given road for a stiff track is not disrupted by the underlying tracks) below 70%.

Overall Tracker Performance

I would like next to discuss the performance of the strawman tracking system in the areas of momentum resolution and impact parameter resolution. To have an intuitive understanding of these critical performance parameters it is useful to develop an analytic approximation to each of them. As it turns out, the impact parameter error is dependent upon the momentum resolution and which is in turn dependent upon the impact parameter measurement.

Momentum Resolution

The momentum resolution of the tracker is in general not a well defined quantity since the tracker has a gaussian response at low (<3-5 GeV/c) and a non-gaussian response with a substantial high momentum tail at higher momenta. It is well known that at higher momentum the measurement is gaussian in the inverse of the momentum which is proportional to the curvature of the track. Thus the high energy tracker performance may be described in terms of a constant σ_p:

$$\frac{dP_\perp}{P_\perp} = \sigma_p P_\perp \quad \text{or} \quad \frac{dP_\perp}{P_\perp^2} = d\left(\frac{1}{P_\perp}\right) = \sigma_p$$

The error in the track curvature can be related to the individual measurement errors of the tracker through a geometric quantity called the sagitta of the track. Figure 10 shows the relationship between the sagitta and the radius of curvature or the track. In the limit that the sagitta, s,is small compared to the measured track length, L, the sagitta is given by :

$$s = \frac{L^2}{8\ R}$$

where R is the radius of curvature of the track. As usual, the radius of curvature can be related to the transverse momentum by :

$$R[m] = \frac{P_\perp[GeV]}{.3\ B[T]\ L[m]^2}$$

and finally the sagitta may be related to $P_\perp$:

$$s[m] = .0375 \frac{B[T]\ L[m]^2}{P_\perp[GeV]}$$

The constant σ_p is just given in terms of the sagitta error, δs, as:

$$\sigma_p = d\left(\frac{1}{P_\perp}\right) = \frac{1}{.0375\ B[T]\ L[m]^2} \quad \delta s$$

Thus the calculation of the momentum resolution at high momenta is reduced to the calculation of the sagitta error. This is most easily done by assuming a three point measurement as shown in Figure 10: one point at the beginning, middle, and end of the track segment. In this case, with the individual errors given by σ_1, σ_2, and σ_3 respectively, the sagitta error becomes:

$$\delta s = \sqrt{\frac{\sigma_1{}^2 + \sigma_3{}^2}{4} + \sigma_2{}^2}$$

Each of the σ_i are weighted averages over several measurement points and depend upon whether one is using the vertex point as a measured point in the fit. Figure 11 tabulates some of the parameters which are used in determining these errors and also the calculated performance parameters. Some of them are also shown here in Table 3. In the case of the vertex fit I assume that there are four high momentum track used to determine vertex position.

Table 3. Tracker resolutions

Fit type	$\sigma_1(\mu m)$	$\sigma_2(\mu m)$	$\sigma_3(\mu m)$	$\delta s(\mu m)$	$\sigma_p(GeV^{-1})$
without vertex (L=.55m)	10	11	30	19	2.1×10^{-3}
with vertex (L=.65m)	11	8	30	18	1.5×10^{-3}

Impact Parameter Resolution

I determine the impact parameter error by using the first and last layers of the silicon to extrapolate the track into the vertex region. The total error is then given by the extrapolation error plus an error due to the uncertainty in the curvature in the track. A diagram is shown in Figure 12. The result is that ($s \ll L$) the impact parameter error, δd, may be expressed as :

$$\delta d^2 = \left[(r+1)\,\delta x_1\right]^2 + \left[r\,\delta x_2\right]^2 + \left[\left(\frac{4R_1}{L}\left(1+\frac{R_1}{L}\right)\right)\delta s\right]^2$$

where δs is the sagitta error, $r = \frac{R_1}{R_2 - R_1}$, L is the track segment length, $R_{1,2}$ are the inner and outer silicon layer radii, and $\delta x_{1,2}$ are the measurement errors for the inner and outer silicon layers. The last term in this expression does not contribution if one knows *a priori* the momentum of the track, as is the case for electrons and muons where the momentum is measured in the EM calorimeter or the muon chamber system.

The final effect on the impact parameter error is the multiple scattering error. This can be characterized as an additional effective measurement error contributing to δx_2 which is momentum dependent, due to scattering in the first and second silicon layers:

$$\delta x_2^{eff\,2} = \delta x_2^{\,2} + \left(\frac{110\mu m}{P_\perp}\right)^2$$

Figure 13 shows the impact parameter versus momentum for the momentum constrained and unconstrained cases. Above 5 GeV the impact parameter resolution is relatively constant at 20μm and 26μm for the respective cases.

An interesting idea would be to use the IPC system alone in the very high luminosity regime ($L=10^{34}cm^{-2}s^{-1}$) and to consider the momentum resolution and impact parameter resolution separately. In this case the IPC will have a high energy impact parameter resolution of 380μm. This will not be useful in locating the event vertex since the beam spot is already much less and would suffice, of order 150μm in the horizontal plane. In this case one can use the inner and outer layers of the IPC system plus the beam spot to

esimate the momentum. The results are shown in Table 3 for the performance parameters to the IPC alone.

Table 2. IPC Performance Paramters when used without the silicon.

Superlayer point resolution	30μm
Sagitta Error	37μm
Sagitta at 1TeV	3μm
$\sigma_p \quad \left(\frac{dP_t}{P_t} = \sigma_p P_t\right)$	14.0×10^{-3} GeV^{-1}
$\sigma_p \left(\frac{dP_t}{P_t} = \sigma_p P_t\right)$ with beam spot (150μm)	6.5×10^{-3} GeV^{-1}
Impact paramter resolution	$\sqrt{(380\mu m)^2 + \left(\frac{600\mu m}{P_t}\right)^2}$

Z Resolution

The Z resolution in the silicon system is determined by the strip pitch (50μm) and the stereo angle in the silicon system. In order to do this one must calculate the RMS resolution of the overlap of two strips, assuming uniform probability across each strip. The result is shown in Figure 14 for both the superlayer and impact parameter resolutions. As one can see, in order to achieve a Z impact parameter resolution below 1mm in the silicon system alone, one would require a stereo angle of greater than 11-12 mrad.

Conclusions

At the moment I would like to refrain from making very definitive conclusions other than that more work is needed to understand how the tracker design, as it stands, effects the physics goals. Gross parameters such as momentum resolution and impact parameter resolution can be easily understood in terms of simple the considerations which I have described above. Understanding the impact of the design on vertex physics is the next major challenge, indeed, understanding the physics of vertex physics is something that requires a good deal of effort in the GEM collaboration.

At the moment, I have not been able to demonstrate the need for a 3 super-layer/9 layer IPC system. At luminosities of $10^{33}cm^{-2}s^{-1}$, the silicon tracker provides the requisite sagitta measurement and vertex measurement so that the IPC system is largely responsible for measuring the outermost point on the track. A four layer measurement would be the most accurate in this case. At luminosities of $10^{34}cm^{-2}s^{-1}$ the momentum resolution of the three superlayer system is inadequate without the vertex point, and the vertex point is best determined by the beam spot. Therefore, only a modest inner superlayer is necessary to measure the sagitta (since the error is dominated by the vertex measurement. It seems that a more cost effective approach might be a two superlayer system with a higher point precision(4 layers, 25μm) on the outside for momentum resolution in conjunction with the silicon system. The inner superlayer could then be two to three layers with a reduced precision of 30-35μm, without a degredation in performance. This will of course require further studies into the pattern recognition capabilities of the tracker.

The issue of whether or not we need a 3-D vertex finding device requires further thought. In principle, the tagging efficiencies of heavy quarks improve dramatically (factors of 2 or more) over the 2-D vertexing system. A simple addition of two layers with large stereo angle strips would be sufficient to do the job. This would most likely not effect the cost by very much and could increase the physics capability substantially.

Appendix 1: Minimum Bias Backgrounds

In this appendix I would like to give the mathematical justification for the minimum bias event statistics. It is not necessarily intuitively obvious that there are on the average 1.6+1=2.6 events per beam crossing in a rare process data sample. We begin by noting that:

$$\sigma_{\text{min bias}} \approx 100\text{mb} \Rightarrow \bar{n}=1.6 \frac{\text{interactions}}{\text{crossing}} \text{ @ } f=62.5\text{MHz}, L=10^{33}/\text{cm}^2\text{s}$$

In addition, the number of interactions per crossing have a Poisson distribution which is given by:

$$P(n)=p(n;\bar{n})=\frac{\bar{n}^n}{n!}e^{-\bar{n}} \quad (n=0,\infty)$$

There are two cases to consider, minimum bias triggers, i.e., at least one minimum bias event, and, rare events which contain a 'Higgs' like process. In either case I calculate the expectation for the average number of events :

Case 1. minimum bias Trigger:

$$P(n)=\frac{p(n;\bar{n})}{1-e^{-\bar{n}}}=\frac{\bar{n}^n}{\left(1-e^{-\bar{n}}\right)n!}e^{-\bar{n}} \quad (n=1,\infty)$$

$$\bar{n}_{\text{min bias}}=\sum_{n=1}^{\infty} nP(n)=\frac{\bar{n}}{1-e^{-\bar{n}}} = 2.0$$

Case 2. Higgs Trigger: let $r=\frac{\sigma_{\text{Higgs}}}{\sigma_{\text{min bias}}}$,

Then for any crossing: $P(\text{Higgs}+n-1 \text{ min bias})=p(n;\bar{n})\cdot r\cdot n=r\cdot n\frac{\bar{n}^n}{n!}e^{-\bar{n}} \quad (n=1,\infty)$

for Higgs triggered sample: $P(n)=n\cdot p(n;\bar{n})=\frac{\bar{n}^{n-1}}{(n-1)!}e^{-\bar{n}}$, $(n=1,\infty$,renormalized)

$$\text{so} \quad \bar{n}_{\text{Higgs}} = \sum_{n=1}^{\infty} nP(n)= \sum_{n=1}^{\infty} n\cdot\frac{\bar{n}^{n-1}}{(n-1)!}e^{-\bar{n}}= \bar{n}+1 = 2.6$$

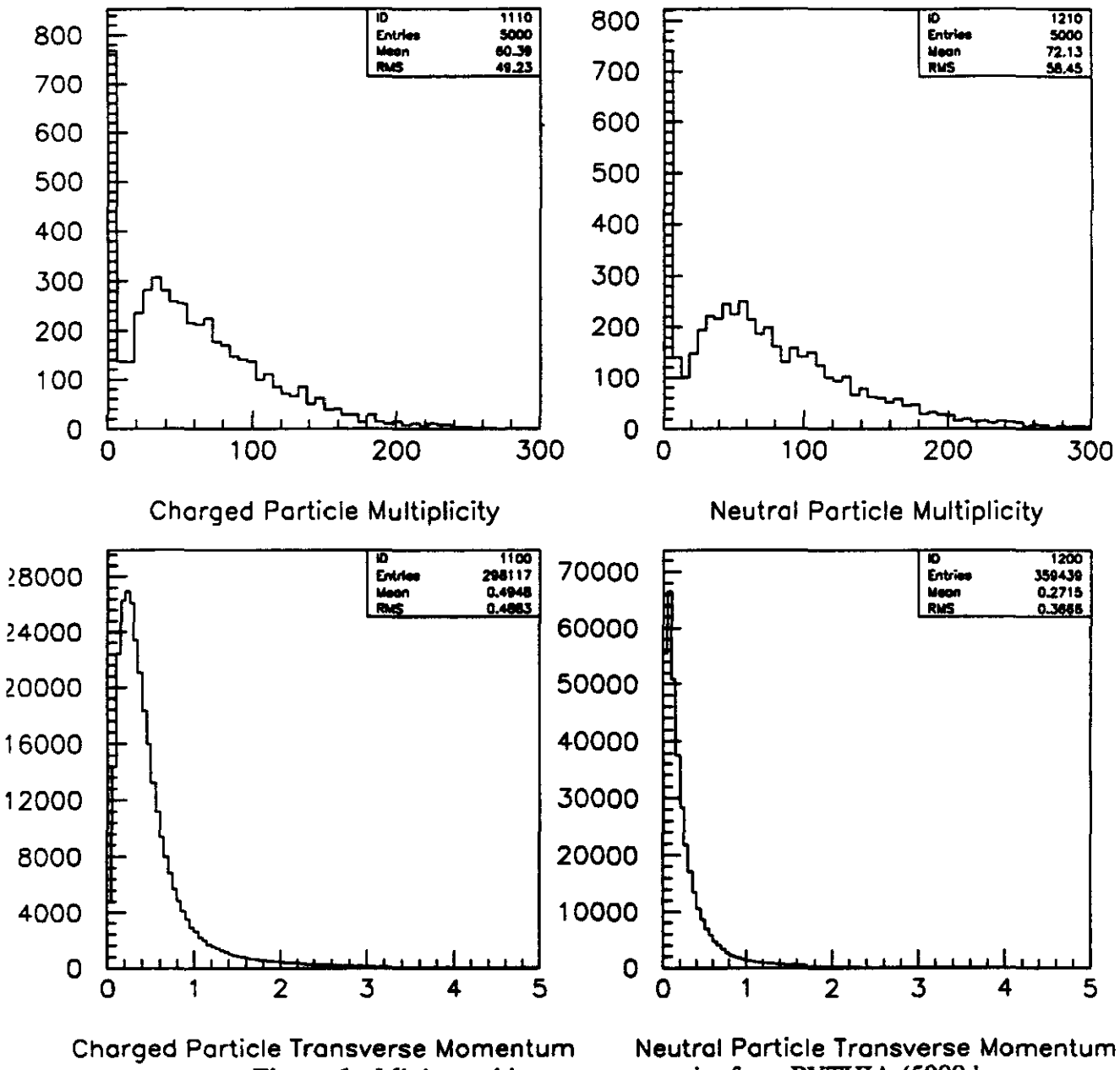

Figure 1. Minimum bias event properties from PYTHIA (5000 beam crossings). Elastic, diffractive, and low P_t have bean included. Charged and neutral particle multiplicities and transverse momentum distributions (neutrinos not included).

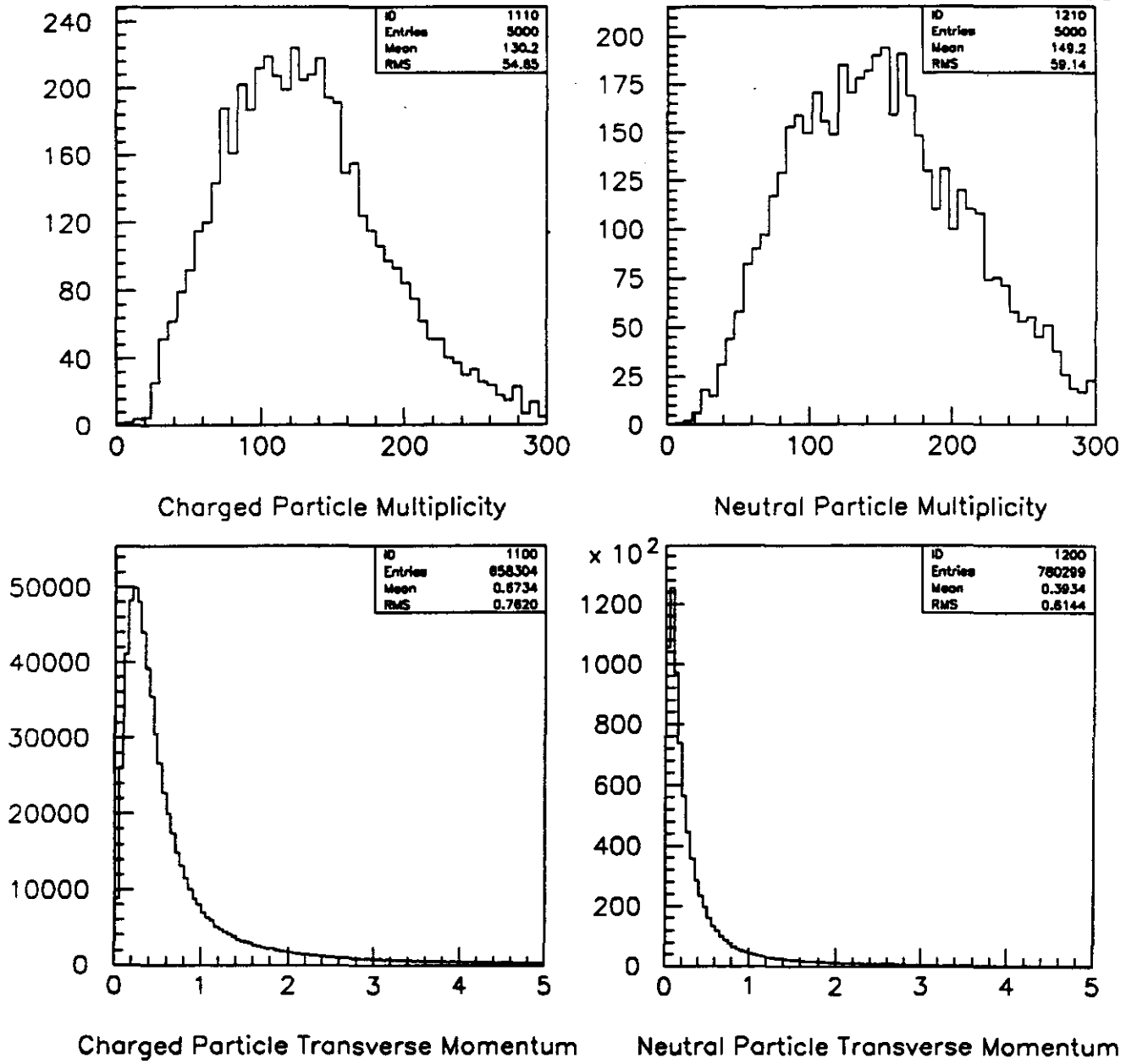

Figure 2. Higgs event properties from PYTHIA (5000 beam crossings). Elastic, diffractive, and low P_t have bean included in addition to the Higgs production with M_H = 300GeV. Charged and neutral particle multiplicities and transverse momentum distributions (neutrinos not included).

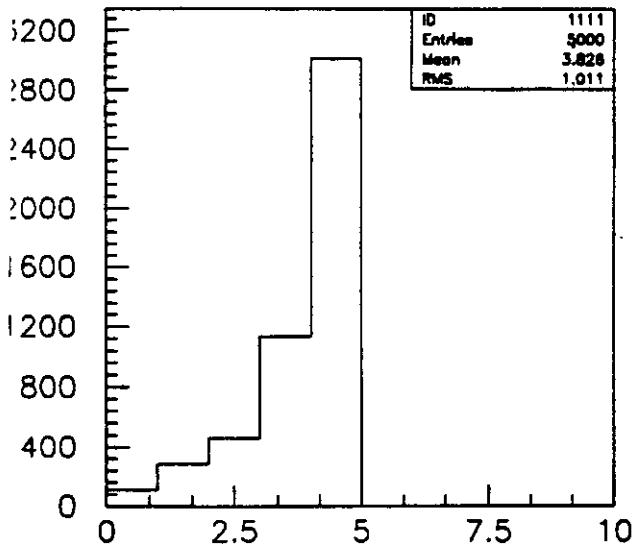

Higgs Daughter Multiplicity

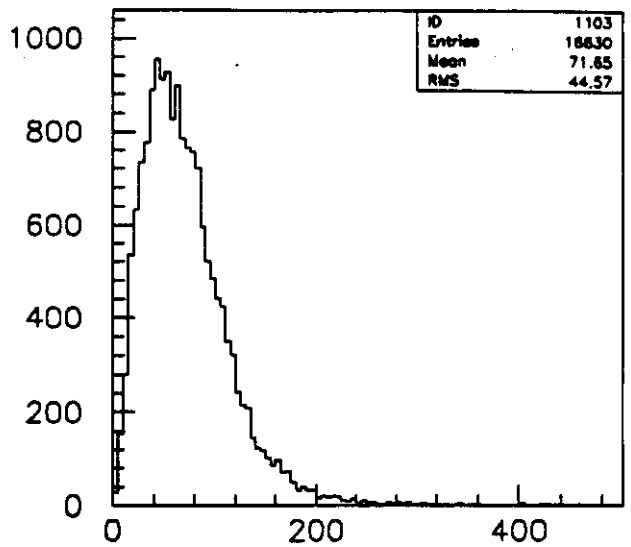

Higgs Daughter Transverse Momentum

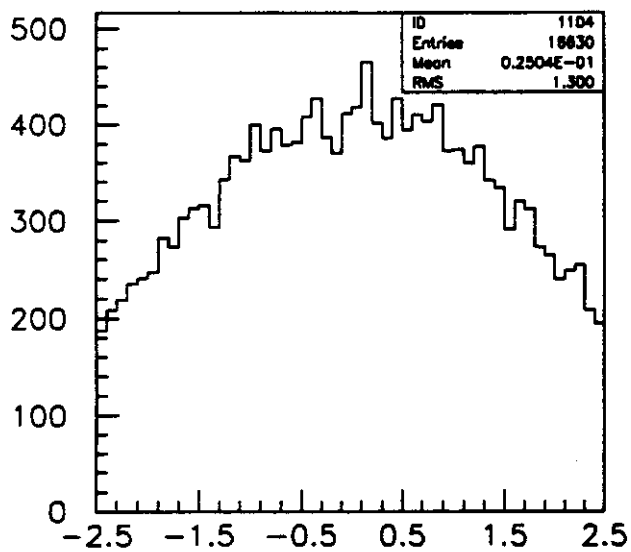

Higgs Daughter Pseudorapidity

Figure 3. Higgs decay product properties from PYTHIA (5000 beam crossings) with M_H = 300GeV, $H_0 \rightarrow Z_0Z_0 \rightarrow$ 4 leptons. The number, the transverse momentum, and the η of the charged leptons found in the interval $-2.5<\eta<2.5$. are plotted above.

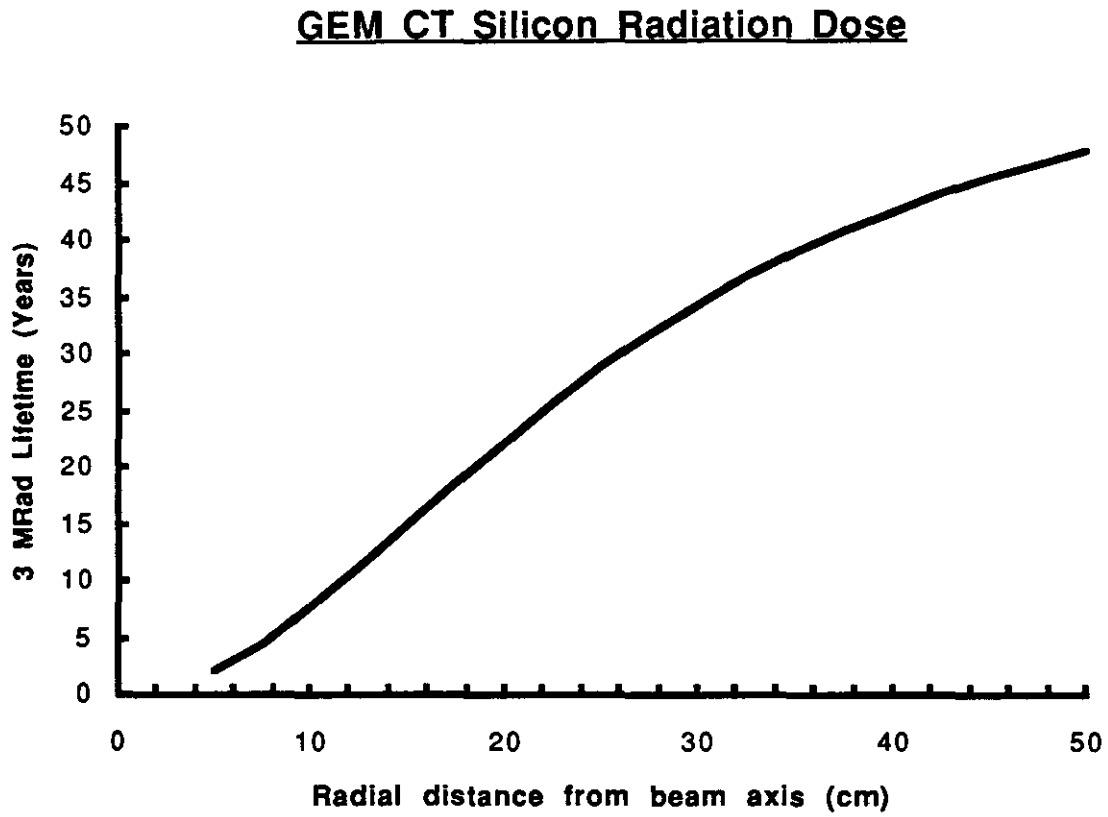

Figure 4. The predicted time to a 3MRad dose as a function of the perpendicular distance from the beam, at η=0, and at a luminosity of $10^{33}cm^{-2}s^{-1}$.

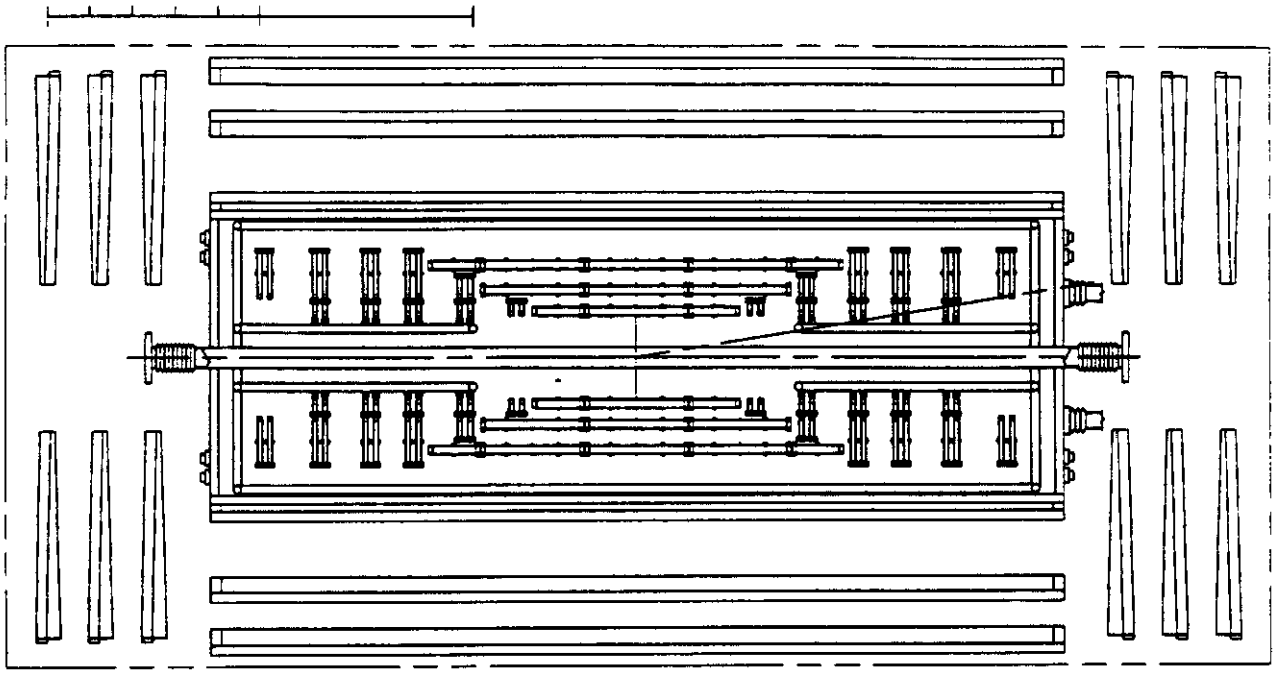

Figure 5. Strawman Central Tracker with Silicon Strip inner tracker and IPC outer tracker. The inner and outer trackers each cover the rapitdity range $-2.5<\eta<2.5$ with three super-layers.

a)

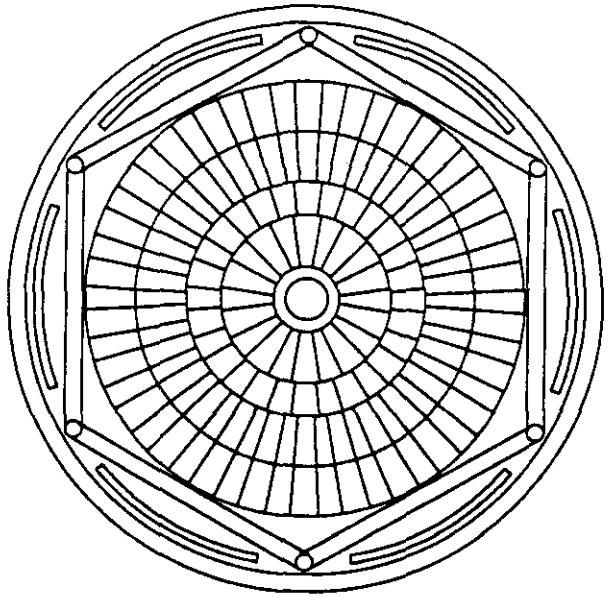

b)

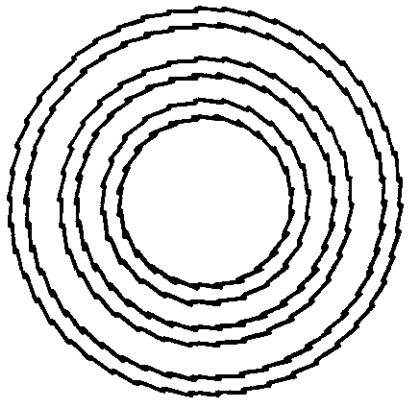

Figure 6. Endviews of the silicon inner tracker. A. Disks in forward region B. Central region barrels

a)

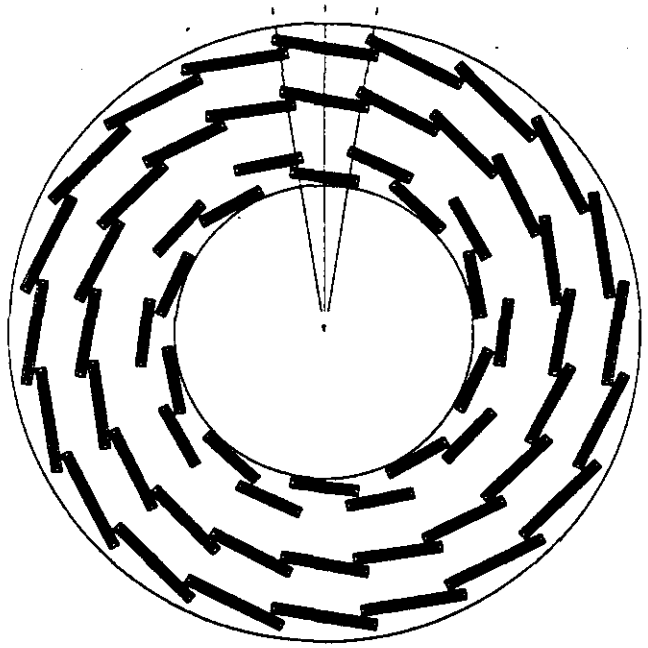

b)

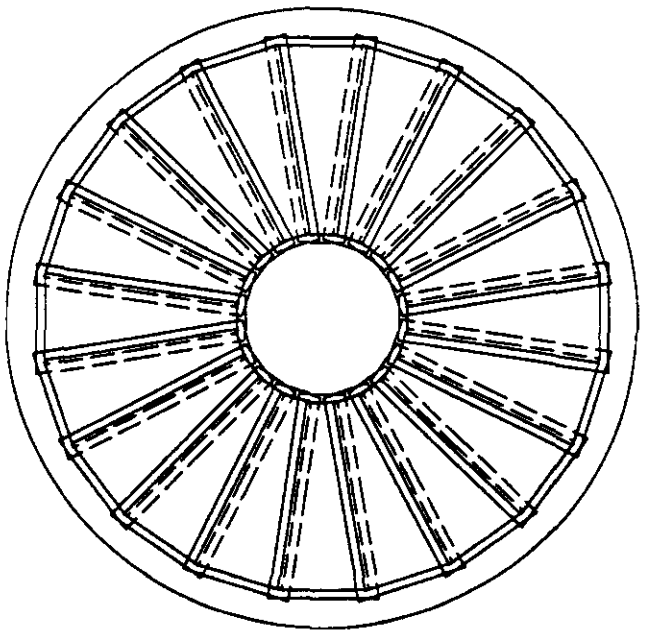

Figure 7. Endviews of the IPC outer tracker. A. Forward region disks B. Central region barrels. Note the staggering of the inner barrel layer due to Lorentz angle considerations.

Minimum Bias Events

Luminosity(/cm^2/s)	1.0E+33
Bunch Frequency	6.25E+07
Luminosity per bunch(mb)	1.60E-02
Minimum bias cross section (mb)	100
Minimum bias events per crossing	1.6
dN/d(eta)d(phi) per MB event	1
Number of Bunches Integrated	1
dN/d(eta)d(phi) per crossing	1.6

Silicon Tracker Occupancies

Notes :
1. all distances in mm
2. Occupancy refers to the average over all minimum bias like beam crossings. It refers to the average number of tracks in a single strip.
3. Space Point Occupancy refers to the average number of tracks in a band around a strip which is covered by the strips 'stereo partner', i.e., an area about 12 times as largeas a single strip.

Silicon Strip Occupancy

Strip Length(mm)	120
Strip width(mm)	0.05
Stereo Angle(radians)	0.006

Bias Occupancy Calculations for Primary Tracks

Barrel Cylinders:

R	Ladder	Z	D(eta)	D(phi)	D(eta)D(phi)	Occupancy	Space Point Occupancy
100	1	0	1.02	5.0E-04	5.1E-04	8.1E-04	9.8E-03
	2	120	0.59	5.0E-04	3.0E-04	4.7E-04	5.7E-03
160	1	0	0.69	3.1E-04	2.2E-04	3.5E-04	4.2E-03
	2	120	0.50	3.1E-04	1.6E-04	2.5E-04	3.0E-03
	3	240	0.36	3.1E-04	1.1E-04	1.8E-04	2.1E-03
220	1	0	0.52	2.3E-04	1.2E-04	1.9E-04	2.3E-03
	2	120	0.42	2.3E-04	9.6E-05	1.5E-04	1.8E-03
	3	240	0.32	2.3E-04	7.4E-05	1.2E-04	1.4E-03
	4	360	0.25	2.3E-04	5.8E-05	9.2E-05	1.1E-03

Forward Disks:

Z	Type	Inner R	Outer R	D(eta)	D(phi)	D(eta)D(phi)	Occupancy	Space Point Occupancy
290	Inner	100	140	3.1E-01	3.6E-04	1.1E-04	1.8E-04	7.1E-04
400	Inner	100	140	3.2E-01	3.6E-04	1.2E-04	1.8E-04	7.4E-04
400	Outer	140	200	3.3E-01	2.5E-04	8.2E-05	1.3E-04	7.9E-04
520	Inner	100	140	3.3E-01	3.6E-04	1.2E-04	1.9E-04	7.5E-04
520	Outer	140	260	5.8E-01	1.9E-04	1.1E-04	1.8E-04	2.1E-03
620	Inner	100	140	3.3E-01	3.6E-04	1.2E-04	1.9E-04	7.6E-04
620	Outer	140	260	5.9E-01	1.9E-04	1.1E-04	1.8E-04	2.2E-03
740	Inner	100	140	3.3E-01	3.6E-04	1.2E-04	1.9E-04	7.6E-04
740	Outer	140	260	6.0E-01	1.9E-04	1.2E-04	1.8E-04	2.2E-03
870	Inner	140	260	6.0E-01	1.9E-04	1.2E-04	1.9E-04	2.2E-03

Figure 8. A tabulation of silicon tracker parameters which includes $\Delta\eta\Delta\phi$ ranges and occupancies for various regions of the silicon tracker. Space point occupancy is defined as the occupancy rate for an unambiguous determination of a space point on the ladder. It is roughly 12 times the single strip occupancy.

IPC Geometry and Occupancy from Primary Tracks:

D(eta)D(phi) for the IPC's	0.001
Number of Crossing Integrated	2
Occupancy	**3.2E-03**
Total Number of Pads (see Below)	**370,635**

Notes:
1. all dimensions in mm
2. All pad sizes are calculated by by assuming a fixed width and then adjusting the length to obtain the requisite D(eta)D(phi) element area.

IPC Pad Size:

Wire Spacing (mm)	2.5
Pad Width	5
Number of Pad Layers per Super Laye	3

IPC Barrel Region:

Barrel Length	2000

Super Layer	R	Pad D(eta)	Pad Length	N Pads in eta	N Pads in Phi	N Pads/Layer
1	370	0.074	27	72	464	100224
2	500	0.1	50	39	628	73476
3	625	0.125	78	25	785	58875
						232575

Total number of Pads in Barrel	232575

IPC EndCap Region:

Inner Radius	200
Outer Radius	700

Super Layer	Z	Inner eta	Outer eta	Eta Divisions	N Pads (x2 Endcaps)
1	1100	2.41	1.23	19	46410
2	1300	2.57	1.38	19	45960
3	1500	2.71	1.51	19	45690
					138060

Total Number of Pads in Endcaps	138060

Figure 9. A tabulation of IPC parameters which includes the number of channels needed to maintain a uniform $\Delta\eta\Delta\phi$=.001. The occupancy from primary tracks is relatively constant for most of the pads.

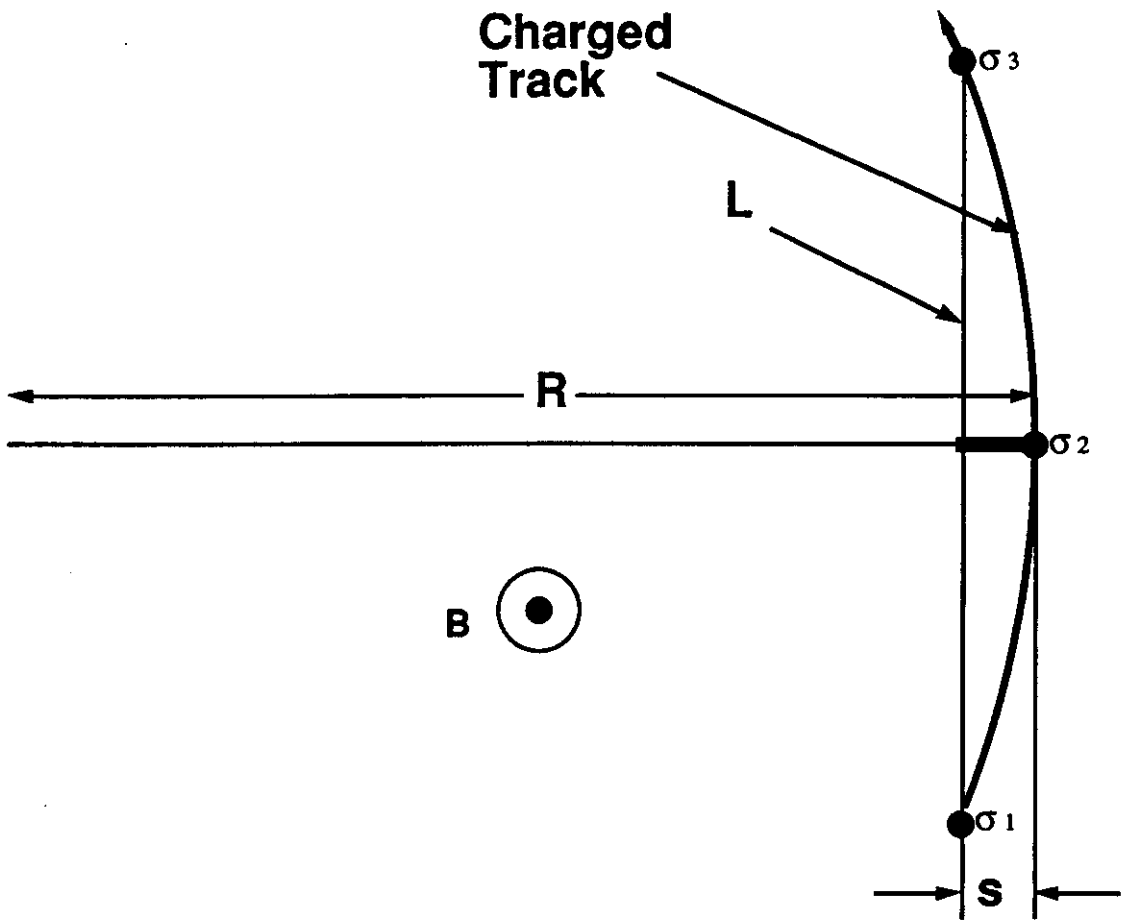

Figure 10. The sagitta, s, of a track segment can be related to the track length, L, and to the radius of curavature, R. R is in turn determined by the magnetic field strength and by the transverse momentum of the particle.

Tracker Performance

Magnetic Field	0 8					
Tracker Geometry						
Silicon Error	0 01					
IPC Error	0 03					
Track Length	550					
Inner Radius	100					
Outer Radius	650					
Tracking Layer	Layer Positions	Point Errors	Effective Sagitta	Effective Sagitta Error	Effective Sagitta	Effective Sagitta Error
Is1	100	0 01	0.00		0.52	0 019
Is2	160	0 01	0.39	0.026	0 74	0 013
Is3	220	0 01	0.68	0.015	0.90	0 011
Ip1	350	0 03	0.99	0.030	0.99	0 030
Ip2	500	0.03	0.79	0.038	0.71	0 042
Ip3	650	0 03	0,00		0.00	
Sagitta Measurement Errors						
Inner Point Error	0.010	0 011				
Mid-Point Error	0.011	0 008				
Outer Point Error	0.030	0.030				
Sagitta Error	0.019					
Sagitta Error (with vertex)	0.018					
Sagitta at 1 TeV(no vertex)	0 009					
Sagitta at 1 TeV(with vertex)	0.013					
dP/P**2(no vertex)	2.14 or for P in GeV		0.0021			
dP/P**2(with vertex)	1.53 or for P in GeV		0.0015			
Impact Parameter Error						
Straight line contribution						
r	0.83					
IP error	0.020					
Curvature error contribution		Multiple Scattering				
Sagitta Error	0.019	Silicon X0/layer	0.006			
IP error	0.017	Theta-0	0.0008			
		Error for third Si point	0.110 /P(GeV)			
Momentum Independent Error	0.026					

Figure 11. A tabulation of tracker performance parameters which includwhich momentum resolution and impact paramter. The impact paramter is calculated by assuming the track momentum (and hence the sagitta) is measured in the entire tracker, while the impact parameter is measured by the silicon system alone.

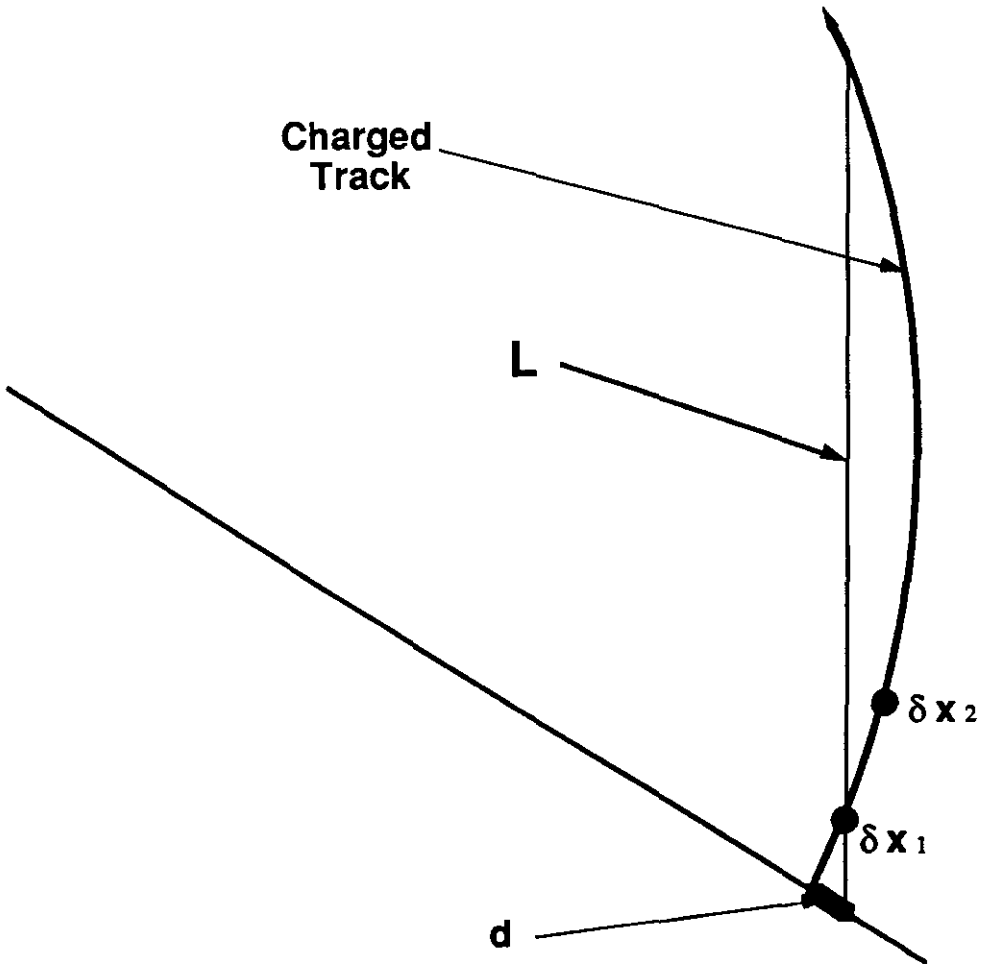

Figure 12. The impact parameter, **d**, of a track to a projected vertex point. The impact parameter is determined by extrapolating into the vertex region with the inner (x_1) and outer (x_2) points in the silicon tracker. The error in the curvature must also be included in the total impact parameter error.

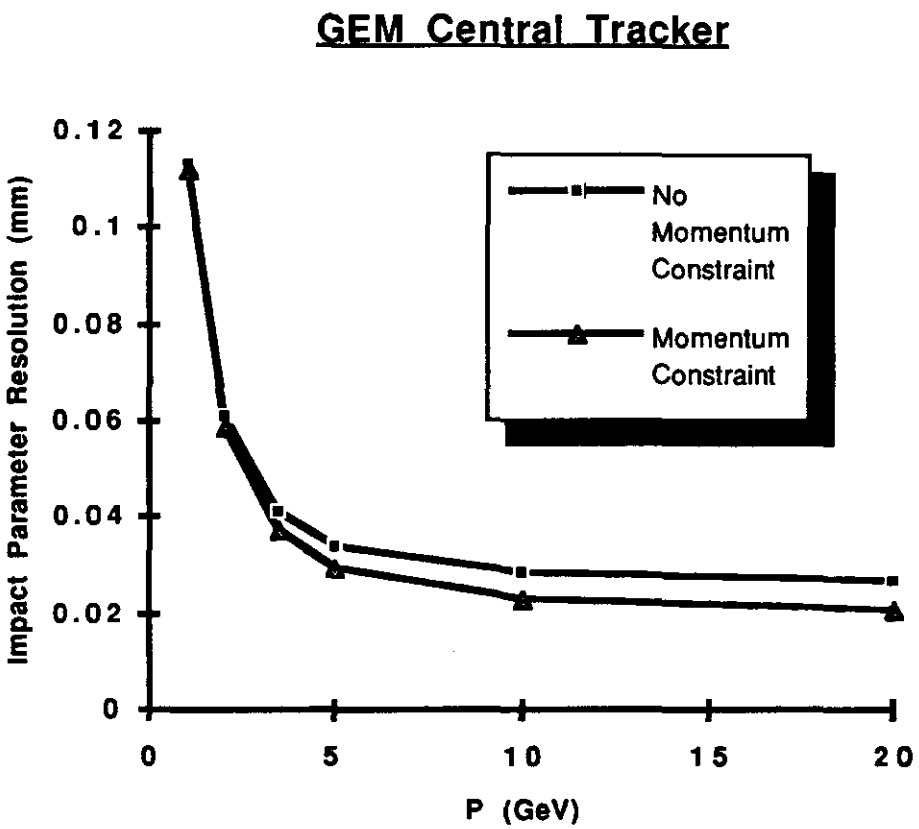

Figure 13. The impact parameter resolution as a function of momentum for a momentum constrained calculation and a momentum unconstrained calculation. The momentum constrained calculation would apply to leptons only where the momentum would be measured i n the calorimeter or muon system.

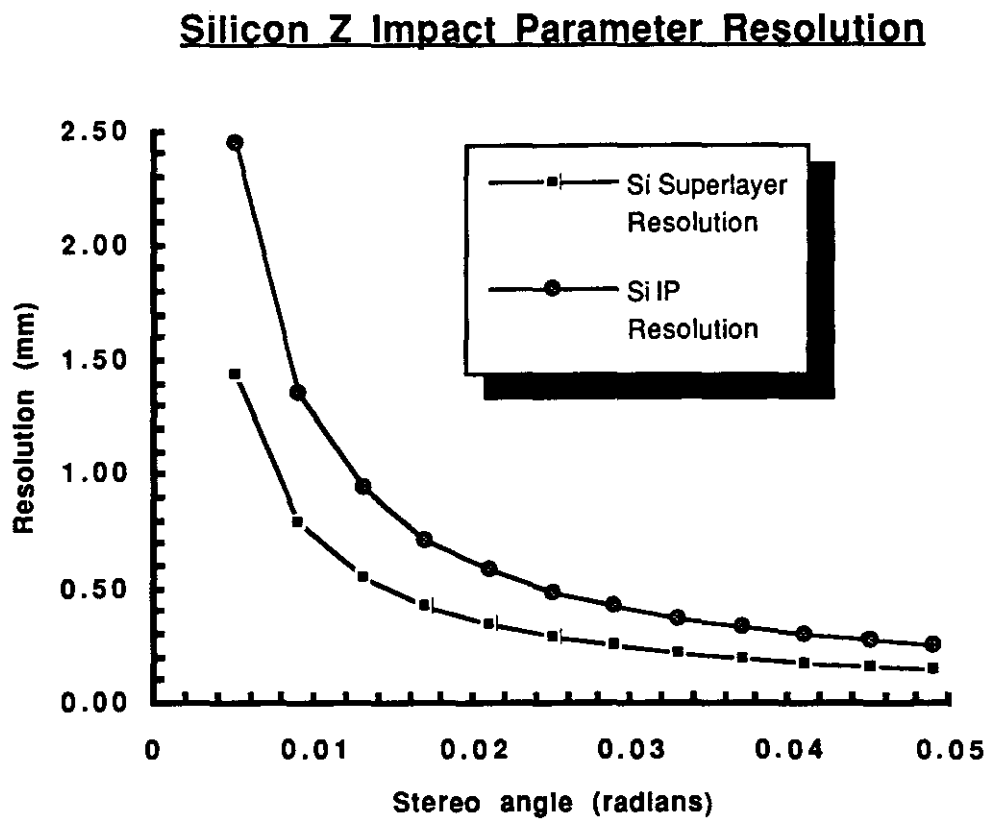

Figure 14. The Z resolution of the silicon as a function of strip stereo angle stereo angle. For an impact parameter resolution better that 1mm one would need a stereo angle of roughly 12 mrad.

---

[1] D Groom et al, 'Radiation in the SSC Interaction Regions', SSC-SR-1033, 18 Feb., 1988

[2] D. Lee, LANL MP-4 , Private Communication

[3] D. Pitzl et al, H. Ziock et al, ...

[4] Kadyk et al, LBL or IEEE I believe...